



ELSEVIER

Journal of Alloys and Compounds 323–324 (2001) 367–371

Journal of  
ALLOYS  
AND COMPOUNDS

www.elsevier.com/locate/jallcom

# Influence of annealing on optical properties of cerium doped soda-lime–silicate glasses

M.A. García<sup>a</sup>, J. Llopis<sup>a,\*</sup>, M.A. Villegas<sup>b</sup>, S.E. Paje<sup>c</sup><sup>a</sup>Departamento de Física de Materiales, Facultad de Ciencias Físicas, Universidad Complutense de Madrid, Ciudad Universitaria, Av. Complutense s/n, 28040 Madrid, Spain<sup>b</sup>Departamento de Vidrios, Instituto de Cerámica y Vidrio, CSIC, 28500 Arganda del Rey, Madrid, Spain<sup>c</sup>Departamento de Física Aplicada, Universidad de Castilla La Mancha, 13071 Ciudad Real, Spain

## Abstract

Effects of annealing on optical absorption (OA) and photoluminescence (PL), emission and excitation spectra from a cerium doped soda-lime–silicate glass ion-exchanged with silver were investigated. Annealing experiments were performed at temperatures of 350 and 400°C, far below the 569°C transition temperature measured for the doped glass. Evidence of surface-plasmon resonance of metallic silver nanoparticles and its subsequent disappearance in the OA spectra by annealing effects are reported. In this case, the reduction of Ag<sup>+</sup> to elemental silver and further reoxidation are governed in part by the reaction  $\text{Ce}^{3+} + \text{Ag}^+ \leftrightarrow \text{Ce}^{4+} + \text{Ag}^0$ . Results are in agreement with a preferential formation of silver nanoparticles at the surface, where the strain energy is more easily relaxed. On the other hand, PL spectra are also affected by the annealing, principally excitation spectra. Analyses of these spectra by de-convolution into three Gaussian shapes were carried out. The influence of annealing has a special significance for the excitation component centered between 3.94 and 3.84 eV (~315 and 323 nm), related to Ce<sup>3+</sup> centers. Superficial increase in the number of Ce<sup>4+</sup> partially prevents excitation of remaining Ce<sup>3+</sup> ions and, therefore, enhances self-absorption in the glass. The main changes in the OA and PL spectral features are discussed in terms of the reducing role of Ce<sup>3+</sup> ions and on the basis of thermal relaxation of the surface tensile stress caused by differences in size between Ag<sup>+</sup> and Na<sup>+</sup> ions. © 2001 Elsevier Science B.V. All rights reserved.

**Keywords:** Luminescence; Light absorption; Optical properties; Amorphous materials

## 1. Introduction

Cerium-containing materials and particularly glasses show a wide range of remarkable properties, which make them essential to a large variety of current applications. These include integrated-optical devices, laser glasses, fluorescent lamps, phosphors, scintillators and many others [1–6]. In these applications, cerium is usually incorporated into the glass network in two oxidation states, Ce(III) and Ce(IV), which ionic equilibrium depends on the conditions of glass formation [7,8]. The Ce(III) is the simplest rare-earth ion with one active *4f* electron, in contrast to the closed shell of tetravalent cerium. Furthermore, it offers a number of characteristic spectral features, which are related to the parity-allowed electric dipole transitions  $5d \leftrightarrow 4f$ . Thus, luminescence in Ce<sup>3+</sup> ions shows broad emission bands in the blue to ultraviolet (UV) region [5],

excitation and absorption spectra in the UV [7–9], short decay times typically of few tens of nanoseconds and UV pulse amplification ability as well as laser-active visible UV transition [10,11]. In contrast, Ce<sup>4+</sup> ions show no luminescence because of the closed shell electronic structure, while the optical absorption appears as a strong charge transfer band peaked in the far UV region.

Further interest in these types of materials derives from the well-established techniques for production of integrated-optical devices. Silver–sodium ion-exchange from molten salts in soda- or soda-lime–silicate glasses is one of the most usual methods for manufacturing these devices because its low cost allows large-scale production. On the other hand, soda-lime–silicate glasses are probably the most widely used and cheapest of all commercial glasses. Therefore, the possibility of forming products based on cerium-containing soda-lime–silicate glasses inexpensively at high speeds seems to be a very promising route. However, knowledge about details of structure rearrangements after silver incorporation by ion-exchange and influence of subsequent annealing is still limited. In this

\*Corresponding author. Tel.: +34-91-394-4495; fax: +34-91-394-4547.

E-mail address: jllolis@eucmax.sim.ucm.es (J. Llopis).

respect, we have recently shown that the optical properties of Ce-doped soda-lime–silicate glass originate in  $\text{Ce}^{3+}$  ions localised in different sites of the glass network [12]. Moreover, the efficient reducing role of  $\text{Ce}^{3+}$  ions on  $\text{Ag}^+$  ions is reflected by a significant drop of the  $\text{Ce}^{3+}$  luminescence together with the rise of the  $\text{Ce}^{4+}$ -charge transfer absorption band when the glass is ion-exchanged with silver. In fact, we have observed by transmission electron microscopy the presence of metallic silver nanoparticles in the glass ion-exchanged at 325°C for periods longer than 1 min.

In the present study, we carried out a systematic analysis of the changes induced by annealing in the optical absorption (OA) and photoluminescence (PL) spectra of Ce-doped soda-lime glass ion-exchanged with silver. Special attention is paid to the formation and stability of metallic nanoparticles of silver against accumulative anneals given to the exchanged samples.

## 2. Experimental

A soda-lime–silicate glass ( $16\text{Na}_2\text{O}\cdot 10\text{CaO}\cdot 74\text{SiO}_2$ ) doped by adding 1 mol% cerium oxide to the batch, was prepared from reagent grade oxides and carbonates. The glass was melted three times at 1550°C under reducing conditions in a gas furnace. After cooling down to room temperature, the ingot was partially cut in samples having dimensions of  $\sim 10\times 10\times 1\text{ mm}^3$ . Then the samples were polished on both sides for OA measurements and subsequently some of them were silver ion-exchanged. For silver–sodium exchange, the samples were immersed in a molten salts bath of molar concentration of 2%  $\text{AgNO}_3$  and 98%  $\text{NaNO}_3$  at 325°C for times ranging from 1 to 10 min.

Annealing experiments were carried out in a tubular furnace at 350 or 400°C for dwell times ranging from 30 to 300 min. Before and after each heat treatment the samples were carefully examined at room temperature by spectroscopic OA and PL. In the former case, the spectra were measured with a Shimadzu 3100 double-beam spectrophotometer over the 220–720-nm range. Likewise, PL experiments were performed in the reflection mode by a Perkin-Elmer LS-5 spectrofluorometer and all the emission (EM) and excitation (EX) spectra were corrected in the 250–720- and 230–700-nm ranges, respectively.

## 3. Results and discussion

### 3.1. Optical absorption

Before the ion-exchange, the glass showed a transparent appearance with a faint yellowish color. Subsequent to ion-exchange and anneals, the color of glass samples changed progressively towards amber coloring with in-

creasing time of ion-exchange and dwell time of annealing. However, the initial yellow coloration can be regained after polishing the surface in a depth of tens of microns. This confirms previous findings about the superficial character of these color variations. The role of silver in these color changes was investigated. For this purpose, two samples, one of them ion-exchanged for 10 min and another unexchanged, were annealed at 400°C in an argon atmosphere for 300 min. The OA of the unexchanged sample exhibited essentially the same spectrum before and after annealing. In contrast, the spectrum of the exchanged sample after annealing displayed an additional defined bell shape band peaked at  $\sim 2.9\text{ eV}$  ( $\sim 425\text{ nm}$ ). This characteristic absorption band has been extensively investigated in silver-containing silicate glasses and it is ascribed to surface-plasmon resonance on metallic nanoparticles of silver [13,14].

In order to be more systematic and clarify these changes of color, we used a series of samples ion-exchanged at 325°C for 1, 3, 5, 7 and 10 min in addition to a reference unexchanged sample. Three accumulative anneals at 350°C for dwell periods of 30 min were performed. Then, the absorption spectrum from every sample of each series, before and after each annealing, was recorded and compared with the others. Prior to the anneals, the absorption spectra of the exchanged samples with respect to that of the reference showed a clear red-shift of the absorption edge of nearly 0.1 eV ( $\sim 10\text{ nm}$ ). In addition, significant increase in intensity over the whole wavelength range was also observed. These increments were more clearly discernible in the visible and near UV region of the spectrum, since above 3.26 eV ( $\sim 380\text{ nm}$ ) the absorption increases rapidly to reach values higher than three. Furthermore, the growth of absorption in the visible and near UV did not show a bell shape and the longer the period of ion-exchange received by the sample, the higher the absorption intensity (Fig. 1). Therefore, the absorption growth in that range is likely a consequence of the rise of inter-valence charge-transfer between  $\text{Ce}^{3+}$  and  $\text{Ce}^{4+}$  ions.

In some step of the annealing, all the exchanged samples exhibited the 2.9-eV band in the OA spectra, which overlapped those related to charge-transfer between  $\text{Ce}^{3+}$  and  $\text{Ce}^{4+}$ . The emergence and growth of the 2.9-eV band and its further diminishing up to its total disappearance by the annealing effect varies from sample to sample as is shown in Fig. 1a–e. Thus, the exchanged sample for 10 min exhibited the most prominent band at 2.9 eV after it underwent the second accumulative anneal (total dwell time of 60 min). Subsequent annealing for an additional 30 min (accumulative dwell time of 90 min) yielded a substantial reduction of the 2.9-eV band. Therefore, the appearance of the 2.9-eV band after annealing and subsequent diminishing is a clear indication that silver nanoparticles were firstly formed in the glass and later disaggregated. In particular, the presence of such nanoparticles depending on the sample and its thermal history,

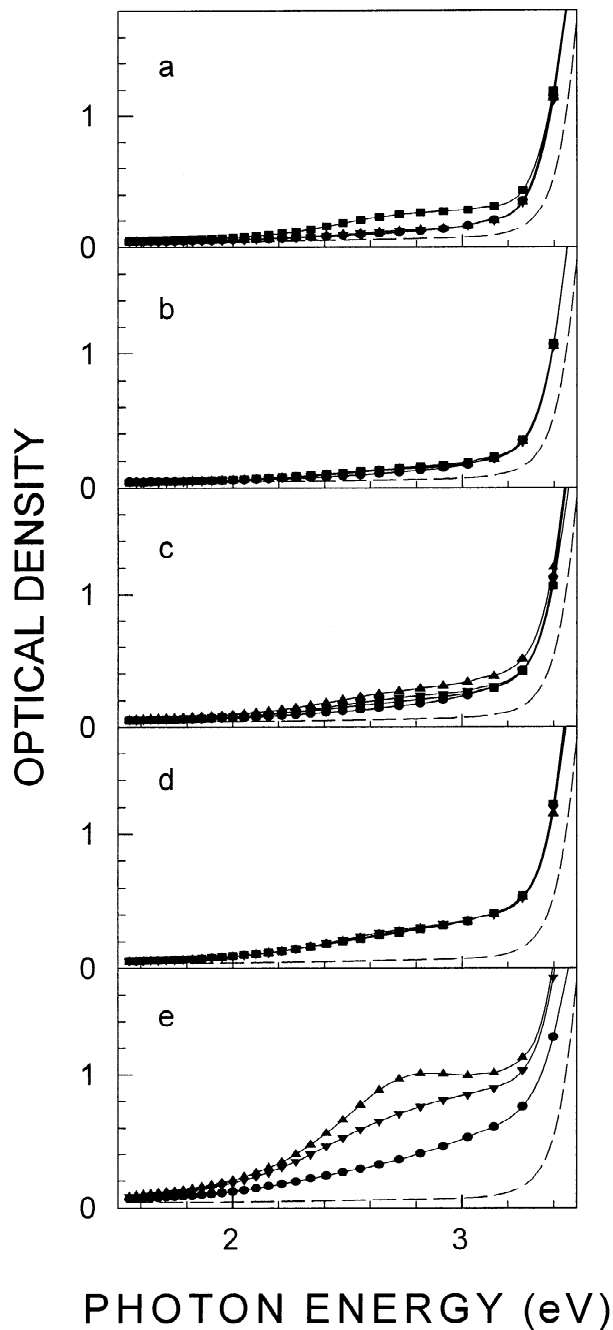


Fig. 1. Optical absorption spectra (dashed lines) from the unexchanged sample and (solid lines) from silver ion-exchanged samples at 325°C for: (a) 1 min, (b) 3 min, (c) 5 min, (d) 7 min and (e) 10 min. Evolution of spectral shape in the visible–near UV range, with accumulative annealing for total dwell time of: (●) 0 min, (■) 30 min, (▲) 60 min and (▼) 90 min, respectively.

strongly suggests that they are induced by thermal relaxation of the surface tensile stress originated by the different size between  $\text{Na}^+$  and  $\text{Ag}^+$  ions. Consequently, it is reasonable that the nanoparticles of silver should be formed mainly at the surface, where the strain energy relaxed more easily. In fact, after the first annealing the

band appeared more prominent in the sample exchanged for 1 min than for the others.

### 3.2. Photoluminescence

The photoluminescent spectral study of the series was performed in parallel with those of absorption. Thus, before and after every annealing, EM and EX spectra of each sample from the two series were recorded and then analysed and compared with the others. Firstly, we analysed the EM and EX spectra from those samples annealed at 400°C for 300 min. Except for variations in intensity, the shapes of the EM spectra before and after annealing were practically coincident. As Fig. 2 shows, the EM spectra under excitation with 3.44-eV ( $\sim 365$  nm) and 3.94-eV ( $\sim 315$  nm) photon energy could be successfully deconvoluted into three and four Gaussian shapes, respectively. In contrast, the EX spectra vary their shapes after annealing. To analyse these changes, the EX spectra were decomposed as a sum of three Gaussian shapes labelled G1, G2 and G3. Thus, the relative intensity of G3 component (peak around 3.94 eV ( $\sim 315$  nm)) for both kinds of samples, increased after annealing as is shown in Fig. 2. Furthermore, the spectra of the exchanged sample

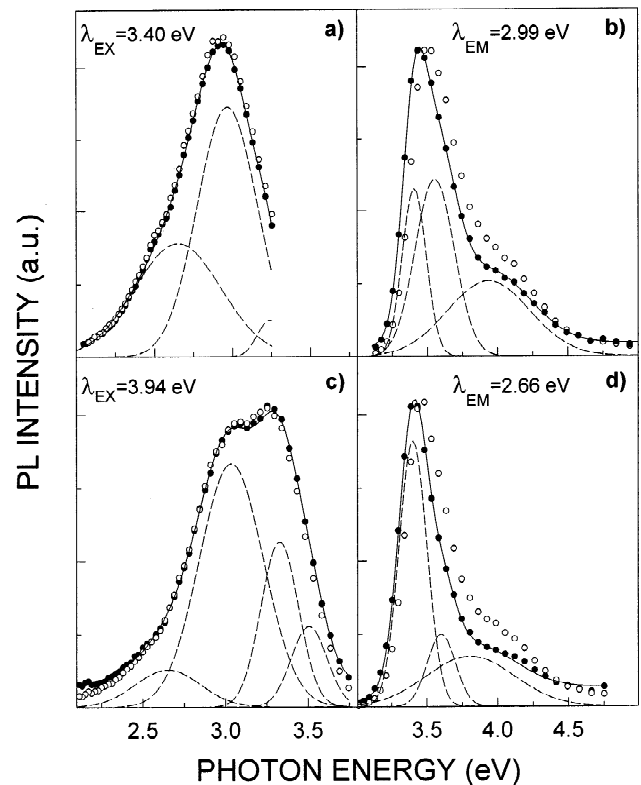


Fig. 2. Normalised PL spectra, deconvoluted into Gaussian shapes, for the unexchanged doped glass (●) before and (○) after annealing at 400°C for 300 min. Emission spectra upon excitation with: (a) 3.40 eV (365 nm) and (c) 3.94 eV (315 nm). Excitation spectra for emission (b)  $\sim 2.99$  eV (415 nm) and (d)  $\sim 2.66$  eV (465 nm).

appeared blue-shifted  $\sim 0.1$  eV with respect to those before annealing, whereas for the unexchanged sample the blue shift was  $\sim 0.05$  eV. The shift of the EX spectra for different emissions can be regarded as an increase of the Stokes shift. This means, therefore, that the loss of stiff surroundings for the active  $\text{Ce}^{3+}$  centers is larger for the exchanged samples. In other words, this is consistent with the presence of nanoparticles of silver and a sort of relaxation in the glass structure in the exchanged samples larger than in the unexchanged one. On the other hand, the G3 component of EX spectra seems to be very sensitive to stress changes in the glass. This is partially supported by the decrease and later disappearance of this component during silver ion-exchange for periods longer than 7 min and its subsequent regain and growth after annealing.

Further systematic analyses of PL spectra from samples of the series annealed at  $350^\circ\text{C}$  for accumulative periods of 30 min were carried out. Since the EM profile spectra were found to be less sensitive to changes in the structure of the glass than the EX profile spectra, we focused the spectral analyses on these latter. Thus, all the EX spectra from the above mentioned series for emission energy at  $\sim 2.99$  eV ( $\sim 415$  nm) and 2.66 eV ( $\sim 465$  nm) were analysed. The spectra could be satisfactorily fitted into the three Gaussian shapes labelled above as G1, G2 and G3, respectively. Main spectral parameters such as peak position, full width at half of maximum (FWHM) and area under the Gaussian shape (so-called integrated intensity) were measured. Fig. 3 shows variations of the peak position and FWHM after every annealing against the exchange time suffered by the sample. As is shown in the figure, major variations of peak position and FWHM appeared from G3 shapes, which ranging from 3.84 to 3.74 eV and 3.96 to 3.84 eV on average for emissions around 2.66 eV and 2.99 eV, respectively. In contrast, the peak position of the G1 component remained constant at  $\sim 3.42$  eV and independent of the emission considered. In any case, we confirm the sensitivity of the G3 component versus silver ion-exchange, that is, with stress changes in the glass. Fig. 4 shows the integrated intensity of the three components in which the EX spectra of the exchanged samples were decomposed, before and after every annealing. As can be seen in the figure, the decrease in intensity for EX components of the emission at  $\sim 2.99$  eV, are sharper than for those at  $\sim 2.66$  eV. As occurred with the other parameters, the G3 component displayed the highest slope value, confirming the high sensitivity of this component to be progressively quenched by the silver ion-exchange. Although for some samples and some specific Gaussian components there was a partial regain in the integrated intensity after a certain anneal (symbols in the figure above the full circles), we can say that the average tendency for the integrated intensity to diminish with increasing exchange time. This means that silver ion-exchange has a detrimental effect on the active  $\text{Ce}^{3+}$  centers which are partially transformed to non-luminescent  $\text{Ce}^{4+}$  ions, according to the following

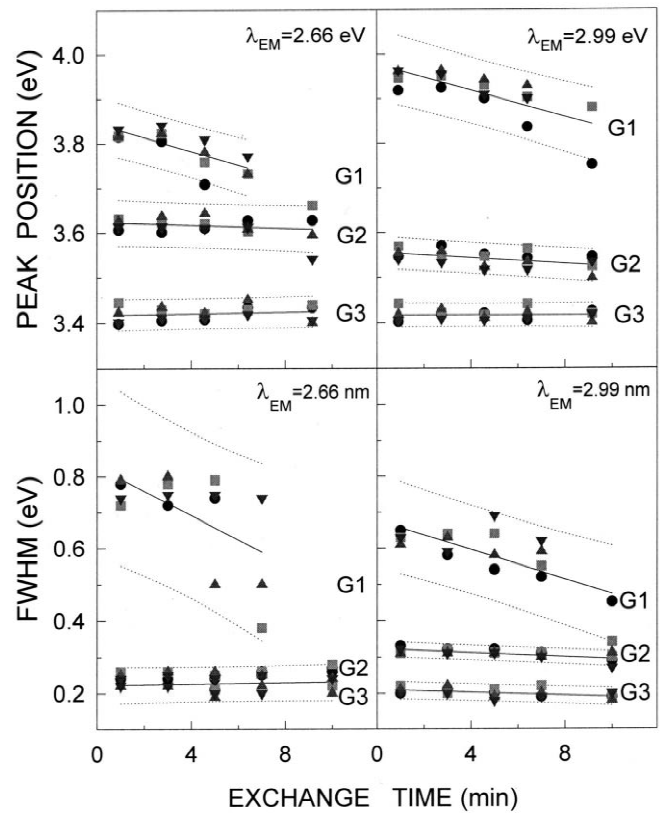


Fig. 3. Peak position and FWHM for each of the three Gaussian shapes in which the EX spectra from the ion-exchanged samples were decomposed. Evolution of both spectral features as a function of exchanged time and after accumulative annealing at  $350^\circ\text{C}$  for total dwell time of (●) 0 min, (■) 30 min, (▲) 60 min and (▼) 90 min, respectively. Solid lines through the symbols represent linear regressions and dotted lines their prediction intervals.

equation:  $\text{Ce}^{3+} + \text{Ag}^+ \rightarrow \text{Ce}^{4+} + \text{Ag}^0$ . In this case, then, the high absorption effectiveness of  $\text{Ce}^{4+}$  ions in the UV region partially prevents the excitation of the non-transformed  $\text{Ce}^{3+}$  ions, in addition to an increasing self-absorption mechanism.

#### 4. Conclusions

In the cerium doped glass investigated, changes in coloration induced by ion-exchange have a superficial character. These changes are related to surface-plasmon resonance on metallic nanoparticles of silver. Annealing experiments show that silver nanoparticles are firstly formed into the glass and later disaggregated. The nanoparticles of silver are induced by thermal relaxation of the surface tensile stress originated by the size difference between  $\text{Na}^+$  and  $\text{Ag}^+$  ions. On the other hand, the OA spectra in the UV range seem to be due to a rise of the inter-valence charge-transfer between  $\text{Ce}^{3+}$  and  $\text{Ce}^{4+}$  ions. Finally, the PL point out that the component of excitation

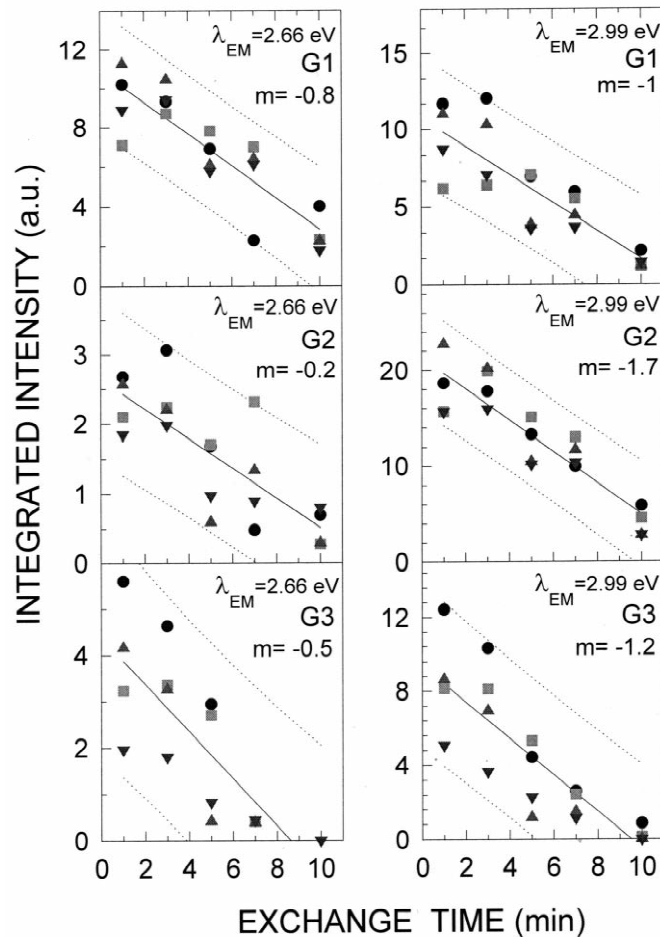


Fig. 4. Integrated intensity for each of the three Gaussian shapes, in which the EX spectra from the exchanged samples were decomposed. Evolution of this spectral parameter as a function of exchanged time and after accumulative annealing at 350°C for total dwell time of (●) 0 min, (■) 30 min, (▲) 60 min and (▼) 90 min, respectively. Solid lines through the symbols represent linear regressions and dotted lines their prediction intervals.

spectra peaked at 3.94 eV is very sensitive to changes in the structure of the glass after annealing.

### Acknowledgements

The authors would like to thank Professor J.M. Fernández Navarro for providing the glasses and suggest their study. We are also grateful to J.J. Vargas (Instituto de Cerámica y Vidrio, CSIC) for his assistance in the preparation of the samples. The financial support of the DGES through project PB97-0287 and EC-FEDER project 2FD97-0141 is gratefully acknowledged.

### References

- [1] S.I. Najafi, in: S.I. Najafi (Ed.) *Introduction To Glass Integrating Optics*, Chapter 6, Atech House, Norwood, MA, 1992.
- [2] C.F. Rapp, in: M.J. Weber (Ed.), *Optical Materials: Part 3, Handbook of Laser Science and Technology*, Vol. V, CRC Press, Boca Raton, FL, 1987, p. 339.
- [3] T.E. Peters, T.G. Pappalardo, R.B. Hunt, in: A.H. Kitai (Ed.), *Solid State Luminescence*, Chapman and Hall, London, 1993.
- [4] G. Blasse, A. Brill, *J. Chem. Phys.* 47 (1967) 5139.
- [5] G. Blasse, B.C. Grabmaier, *Luminescent Materials*, Springer, Berlin, 1994.
- [6] C. Dujardin, C. Pedrini, W. Blanc, J.C. Gâcon, J.C. Van't Spijker, O.W.V. Frijns, C.W.E. van Eijk, P. Dorenbos, R. Chen, A. Fremout, F. Tallouf, S. Tavernier, P. Bruyndonckx, A.G. Petrosyan, *J. Phys. Condens. Matter.* 10 (1998) 3061.
- [7] J.S. Stroud, *J. Chem. Phys.* 35 (1961) 844.
- [8] J.A. Duffy, G.O. Kyd, *Phys. Chem. Glasses* 37 (1996) 45.
- [9] A. Paul, M. Mulholland, M.S. Zaman, *J. Mater. Sci.* 11 (1976) 2082.
- [10] Y. Ishii, K. Arai, H. Namikawa, M. Tanaka, A. Negishi, T. Handa, *J. Am. Ceram. Soc.* 70 (1987) 72.
- [11] N. Sarukura, Z. Liu, Y. Segawa, K. Edamatsu, Y. Suzuki, T. Itoh, V.V. Semashko, A.K. Naumov, S.L. Korableva, R.Yu. Abdulsabirov, M.A. Dubinskii, *Optics Lett.* 20 (1995) 294.
- [12] S.E. Paje, M.A. García, M.A. Villegas, J. Llopis, *Opt. Mater.* (in press).
- [13] U. Kreibig, M. Vollmer, *Optical Properties of Metal Clusters*, Springer, Berlin, 1995.
- [14] E. Borsella, G. Battaglin, M.A. García, F. Gonella, P. Mazzoldi, R. Polloni, A. Quaranta, *Appl. Phys. A* 71 (2000) 125.